Autonomous Information Gathering Guidance for Spacecraft-to-Spacecraft Tracking with Optical Sensors

Jesse Greaves
University of Colorado Boulder
Daniel Scheeres
University of Colorado Boulder

ABSTRACT

Spacecraft to spacecraft absolute tracking has the potential to enable autonomous navigation for a space system seeking to provide space domain awareness by observing other resident space objects. Spacecraft to spacecraft absolute tracking is a method of estimating the absolute states of the observed objects and the observer simultaneously, and this method is feasible with optical-only sensors. While optical sensors allow cooperative and non-cooperative tracking, they lack immediate range information which may lead to large associated uncertainties. To ensure accurate tracking, maneuvers can be employed to gather state information. To reduce operational complexity, and fuel use, information gathering maneuvers can be combined with station keeping. This paper combines these operations by projecting the information gathering maneuvers into the station keeping set to achieve desired states with minimal range uncertainty. The results of this method are simulated in cislunar space, and show the desired state targeting and information gathering capabilities.

1. INTRODUCTION

Space Domain Awareness (SDA) is necessary to ensure universal security and performance of space born systems. Without adequate observational resources conjunction events and navigation errors become plausible sources of mission failure. The need for an enhanced observational capacity to meet the current SDA demand is becoming increasingly evident due to the expanding deployment of space systems which are overburdening traditional ground-based assets. To guarantee the continued safe use of space, observational capabilities must be able to manage the growth in resident space objects, which warrants the investigation of autonomous observation platforms which can track objects without intervention.

One promising approach to augment observational abilities is through the development of space-based observation platforms for spacecraft-to-spacecraft absolute tracking (SSAT). Space-based platforms are significantly more versatile compared to their ground-based counterparts and avoid limitations such as stagnant viewing geometries, atmospheric occlusion, and passive observing. Removing these limitations are particularly pertinent and beneficial for spacecraft wandering further from Earth's sphere of influence, such as cislunar missions which are receiving considerable attention due to various international programs aimed at inhabiting lunar space. In addition, the methodology of SSAT enables simultaneous state estimation of the observer and target which enables fully autonomous tracking so that it does not require costly or timely operator intervention. The primary drawback to this approach is that it relies heavily on non-linearities in the dynamics of the system to obtain information on the entire state, which can prove challenging for conventional filters. Overall SSAT has the potential to robustly bolster observational competency to handle the expected growth of resident space objects in the foreseeable future.

To maximize the benefit of a space-based observation platform, the observer should be able to measure cooperative and non-cooperative targets. Measurements of this type are an essential tool for an SDA asset since tracking space debris or other non-communicative bodies is a vital objective. One such sensor that can achieve this is an optical sensor. Optical sensors are ideal for SDA because they are cheap, readily available, have an abundance of supportive literature, and do not require cooperation. The major associated drawbacks with optics are limited range information and lighting constraints. The limited range information associated with optical sensors in combination with the challenges

associated with SSAT provide motivation to increase information gain and reduce state uncertainty and improve filter performance. Fortunately, state information can be gained through the application of properly designed maneuvers which set up relative dynamics conducive to increasing information content. This motivates the primary objective of this work which is to design an autonomous guidance algorithm to improve observational abilities for SSAT using optical sensors.

2. BACKGROUND

2.1 Spacecraft to Spacecraft Absolute Tracking

Spacecraft to spacecraft tracking has a significant collection of background literature and applications. While extensive, we focus here on SSAT, which is the use of relative measurements between space objects to generate an absolute/global state estimate for the distributed space system. SSAT literature originates with F.L. Markley who proved the SSAT problem is fully observerable near Earth if the orbit period, eccentricity, and phasing are not matched between relative orbits [17]. Subsequently, M.L. Psiaki showed the J2 gravity harmonic further improved observability [22]. Later still, K.A. Hill examined SSAT in cislunar space to demonstrate the utility of SSAT for interplanetary missions [12]. Contemporary works expanded on these results by further exploring a variety of use cases with various measurement sensors and dynamical environments [20, 16, 2, 25, 7].

In addition to estimating the absolute state from relative measurements, the full relative state must also be observable which is not guaranteed for single sensor systems. Specifically, obtaining range information from optical-only measurements under linear dynamics is unobservable. Fortunately, it has recently been shown that range is locally observable with optics for specific nonlinear orbital motions, in that there are unique configurations in which range information can be obtained if relative orbits are appropriately designed [13, 23, 25, 27, 6, 15]. As a result, it is possible for optical-only measurements to produce complete observability for both the absolute and relative states of a distributed space system. Even though this is theoretically feasible, there are configurations in which range information is difficult to obtain, and therefore methods to gather information on the range state is pertinent to examine.

2.2 Information Gathering for Optics

The concept of information gathering is especially important for systems which are slow to accrue information, such as single sensor systems like optical-only measurements. Optical-only measurements, also commonly referred to as angle-only or bearing-only measurements, are appealing because they generally use lightweight, low cost, and widely available technology with an abundance of literature and application. The primary weakness is that they lack range information, which can lead to observability issues in linear systems [19, 28]. Optical-only observability has been studied at length for various systems, and while some systems may be observable, there is a general consensus that obtaining range information is always an important consideration [10, 11, 21, 14, 4].

Optical-only observability and tracking is an influential problem for space systems because optical sensors are often a primary measurement for relative spacecraft operations and space domain awareness. Because of this, methods for obtaining range information during spacecraft proximity operations has been well studied in low Earth orbit. D.C. Woffinden proved that under linerized motion optical-only measurements cannot produce range observability [28]. To combat the lack of range information, Woffinden and J. Grzymisch went on to develop optimal maneuvers to gather the necessary information [29, 9]. Since then, work extending maneuvers to optimize range information has been advanced in to new environments, such as cislunar space, with a variety of solutions [3, 5, 26, 18]. Crucially, the previous works either provide a non-generalizable solution specific to a single scenario, or nonlinear solution that is costly to compute. Additionally, all of the works assumed a well-known target state and are not as easily adopted into the SSAT setting. Recent work has shown that there are heuristic guidance policies and surrogate cost function which are suitable for autonomous information gathering guidance in any setting [8]. This paper will utilize the maximum measurement deviation guidance policy developed in that work and combine it with station keeping objectives to minimize spacecraft operations.

3. PROBLEM FORMULATION

3.1 Spacecraft to Spacecraft Absolute Tracking Model

The spacecraft to spacecraft absolute tracking problem estimates the state of multiple objects in a distributed system while only relying on relative measurements between them. This work only considers two vehicles; an agent which is

actively managed and a target which is nominally non-cooperative. Let $\boldsymbol{s}_a \in \mathbb{R}^n$ be the state of the agent in the dynamic reference frame which motion is calculated. This agent is responsible for generating measurements and is actively managed. Then let $\boldsymbol{s}_t \in \mathbb{R}^n$ be the state of the target in the dynamic reference frame, which operates independently of the agent so that cooperative planning is not required for this architecture. Because the SSAT problem seeks to provide state estimates for both vehicles, the dynamic SSAT system state is comprised of both the target and the agent sub-states and is defined by:

$$\boldsymbol{x} = \begin{bmatrix} \boldsymbol{s}_a^T & \boldsymbol{s}_t^T \end{bmatrix}^T \tag{1}$$

Estimating the dynamic state of both vehicles is equivalent to estimating a relative and absolute state simultaneously. A relative SSAT system state containing absolute and relative partitions is now defined:

$$\tilde{\boldsymbol{x}} = \begin{bmatrix} \boldsymbol{s}_\alpha^T & \boldsymbol{s}_\rho^T \end{bmatrix}^T \tag{2}$$

Explicitly defining an absolute and relative state enables user to more easily identify relative information which is important to information gathering later. To fully define the relative system the sub-states are now defined. First, let the absolute state be defined as the mean of the vehicles and the relative state be the difference from the agent to the target as in:

$$\boldsymbol{s}_\alpha = \frac{\boldsymbol{s}_a + \boldsymbol{s}_t}{2} \tag{3}$$

$$\boldsymbol{s}_\rho = \boldsymbol{s}_t - \boldsymbol{s}_a \tag{4}$$

Defining the absolute and relative sub-states in such a manner leads to a simple linear transformation between the inertial and relative SSAT systems, as well as simplifications which provide insight into observability properties. Though in practice it may be easier to implement a different relative system, such as an agent based absolute state, the observability properties from this analysis will still apply. In fact, we will provide an agent based absolute state later to demonstrate its equivalence and usage.

From the definitions of the states above there is a linear transformation $\boldsymbol{T}$ from the inertial SSAT state $\boldsymbol{x}$ to the relative SSAT state $\tilde{\boldsymbol{x}}$, such that:

$$\tilde{\boldsymbol{x}} = \boldsymbol{T}\boldsymbol{x} \tag{5}$$

$$\boldsymbol{T} = \begin{bmatrix} \frac{1}{2}\boldsymbol{I}_{n\times n} & \frac{1}{2}\boldsymbol{I}_{n\times n} \\ -\boldsymbol{I}_{n\times n} & \boldsymbol{I}_{n\times n} \end{bmatrix} \tag{6}$$

The linear transformation $\boldsymbol{T}$ is a linear mapping between dynamic and relative states, and therefore it can also map associated state estimates. If the SSAT system is estimated with a Gaussian uncertainty model, with the covariance of the dynamic estimate being $\boldsymbol{P}$, then the transformation to the relative uncertainty is:

$$\tilde{\boldsymbol{P}} = \boldsymbol{T}\boldsymbol{P}\boldsymbol{T}^T \tag{7}$$

3.2 Dynamical Model

With the state defined, the spacecraft equations of motion can now be incorporated. The natural dynamics model that dictates motion is given by the function $\dot{\boldsymbol{s}}_i = \boldsymbol{f}(\boldsymbol{s}_i)$. Therefore, the inertial state dynamics are:

$$\dot{\boldsymbol{x}} = \begin{bmatrix} \boldsymbol{f}(\boldsymbol{s}_a)^T & \boldsymbol{f}(\boldsymbol{s}_t)^T \end{bmatrix}^T \tag{8}$$

Spaceflight dynamics is modeled as a second order ordinary differential equation and therefore position and velocity are required to integrate the state. Thus, let the dynamic state be composed of position and velocity vectors be given by the vectors $\boldsymbol{r}_i \in \mathbb{R}^3$ and $\boldsymbol{v}_i \in \mathbb{R}^3$, where the subscript i is denotes the spacecraft. Then the state dynamics are:

$$\boldsymbol{f}(\boldsymbol{s}) = \begin{bmatrix} \boldsymbol{v}^T & \boldsymbol{a}^T \end{bmatrix}^T \tag{9}$$

$$\tag{10}$$

where $\boldsymbol{a}_i$ is the acceleration given by the equations of motion.

This work is interested in cislunar motion, which is approximated using the circular restricted three body problem (CR3BP). The restricted assumption is that the third body's mass is negligible compared to the two primary bodies and does not impact their motion. When the restricted assumption is true then the two massive bodies will follow an analytic two body solution, and the third body will have its motion dictated by their positions. The circular assumption is that the two massive bodies are in circular orbits about their barycenter. From this setting, the acceleration in the CR3BP is:

$$\boldsymbol{a} = -2[\tilde{\boldsymbol{\omega}}_{D/N}]\boldsymbol{v} - [\tilde{\boldsymbol{\omega}}_{D/N}][\tilde{\boldsymbol{\omega}}_{D/N}]\boldsymbol{r} - \frac{Gm_1}{\rho_{b1}^3}\boldsymbol{\rho}_{b1} - \frac{Gm_2}{\rho_{b2}^3}\boldsymbol{\rho}_{b2} \tag{11}$$

$$\boldsymbol{\omega}_{D/N} = \sqrt{\frac{G(m_1+m_2)}{r_{12}^3}}\hat{\boldsymbol{e}}_z \tag{12}$$

In this equation r_{12} is the distance between the massive bodies and $\boldsymbol{\omega}_{D/N}$ is the angular rotation rate vector of the CR3BP rotating frame (the dynamical frame D) with respect to the inertial frame (N). The parameters m_1, m_2 are masses of the primary bodies, and $\boldsymbol{\rho}_{b1}$ and $\boldsymbol{\rho}_{b2}$ are the vectors from the bodies to the spacecraft $\boldsymbol{r}$. A diagram of the CR3BP is in Figure 3.2.

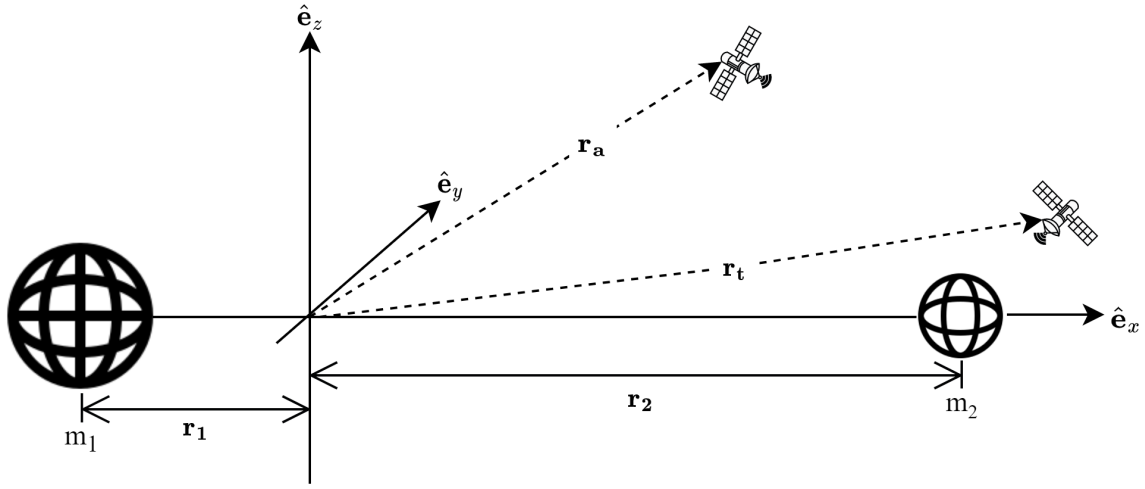

Fig. 1: Diagram of the circular restricted three body problem.

We equip the agent spacecraft with the capability to execute control in the form of impulsive velocity changes. Control is denoted by the vector $\boldsymbol{u} \in \mathbb{R}^p$ and influences the state through the agent's control input matrix $\boldsymbol{B}_a$. The discontinuous state before and after the impulse is $\boldsymbol{x}^-$ and $\boldsymbol{x}^+$ respectively. The state equations for control are:

$$\boldsymbol{x}^+ = \boldsymbol{x}^- + \boldsymbol{B}_a\boldsymbol{u} \tag{13}$$

$$\boldsymbol{B}_a = \begin{bmatrix}\mathbf{0}_{3\times3} & \boldsymbol{I}_3 & \mathbf{0}_{3\times3} & \mathbf{0}_{3\times3}\end{bmatrix}^T \tag{14}$$

Control is limited to the agent vehicle, and because we are examining agent guidance policies, we do not include control execution errors to determine the policies ideal performance. In application there will be execution errors, but because the agent is cooperative it should have access to accelerometers which can measure errors. Other works have shown that with a sufficient accelerometer then maneuvers can be effectively used to improve state estimation [26].

3.3 Measurement Model

Optical measurements are represented in many ways, but one common method is an azimuth and elevation angle pair as given by:

$$\theta_a = \tan^{-1}\left(\frac{\rho_y}{\rho_x}\right) \tag{15}$$

$$\theta_e = \sin^{-1}\left(\frac{\rho_z}{\rho}\right) \tag{16}$$

$$\boldsymbol{y}_\theta = \begin{bmatrix}\theta_a & \theta_e\end{bmatrix}^T \tag{17}$$

By using the above representation we are assuming that there is a separate image processing system has identified the target and converted the image data into the dynamic reference frame via necessary frame rotations and transformations. The sensitivity of these measurements with respect to the relative state vector, denoted as $\boldsymbol{H}_\theta$, is:

$$\boldsymbol{H}_\theta = \begin{bmatrix} \frac{-\rho_y}{\rho_x^2+\rho_y^2} & \frac{\rho_x}{\rho_x^2+\rho_y^2} & 0 & \boldsymbol{0}_{1\times 3} \\ \frac{-\rho_x\rho_z}{\rho^2\sqrt{\rho_x^2+\rho_y^2}} & \frac{-\rho_y\rho_z}{\rho^2\sqrt{\rho_x^2+\rho_y^2}} & \frac{\sqrt{\rho_x^2+\rho_y^2}}{\rho^2} & \boldsymbol{0}_{1\times 3} \end{bmatrix} \tag{18}$$

Measurements are taken once an hour with a zero mean Gaussian noise model. The measurement covariance is determined by a root-mean-square uncertainty model to account for partially resolved object uncertainty. The root-mean-square model combines a minimum angular uncertainty parameter $\sigma_{\theta,min}$ with a reference resolution uncertainty parameter D. The equation for the angular uncertainty model is:

$$\rho^2\sigma_\theta^2 = \rho^2\sigma_{\theta,min}^2 + D^2 \tag{19}$$

$$\sigma_\theta = \sqrt{\sigma_{\theta,min}^2 + \frac{D^2}{\rho^2}} \tag{20}$$

The minimum angular uncertainty parameter accounts for all pointing errors, including spacecraft attitude errors which are not directly modeled. The value of $\sigma_{\theta,min}$ is set to 10 micro-rad, which was chosen to emulate a high accuracy sensor based on Reference [1]. The resolution uncertainty D is 4 meters, which is approximately half the size of Lunar Gateway modules [24]. Note that even though these uncertainties are small, they are obtainable, and reducing the accuracy will only reduce state accuracy results but will not invalidate the methods applied. Additionally, we neglect any sensor limitations because we are seeking to identify ideal performance and because the close proximity operations that will ensure that the two spacecraft always have line-of-sight.

3.4 Analytic Information Gathering

This work is specifically building off of Reference [8] for information gathering guidance policies which minimize range uncertainty for optical sensors. The cost function which was minimized in the previous work is the variance of the range estimate given by:

$$J_\rho(\boldsymbol{u}) = \boldsymbol{M}_\rho^T\tilde{\boldsymbol{P}}_f\boldsymbol{M}_\rho \tag{21}$$

$$\boldsymbol{M}_\rho = \begin{bmatrix}\boldsymbol{0}_{n\times 1}^T & \hat{\boldsymbol{\rho}}_{\tau_f}^T & \boldsymbol{0}_{(n-3)\times 1}^T\end{bmatrix}^T \tag{22}$$

where $\boldsymbol{\rho} = \boldsymbol{r}_t - \boldsymbol{r}_a$ is the relative range vector from the agent to the target.

To minimize the cost function the previous work presented two guidance policies for autonomous operations. First, there was a heuristic policy which was to maneuver perpendicular to the line of sight. This policy contained the optimal maneuver for short coasting periods, but is an admissible control set which is not directly applicable to guidance. Then a surrogate cost function was proposed to a maximize measurement deviation (MMD), which produced an analytic and nearly optimal policy which is the solution to an eigen-problem. The MMD policy is given by:

$$\boldsymbol{u}_y = \pm\upsilon\max(\text{eig}(\boldsymbol{Q})) \tag{23}$$

$$\boldsymbol{Q} = \boldsymbol{B}_a^T\boldsymbol{\Phi}(\tau_f,\tau_0)^T\boldsymbol{H}_f^T\boldsymbol{H}_f\boldsymbol{\Phi}(\tau_f,\tau_0)\boldsymbol{B}_a \tag{24}$$

where υ is the maximum allowable control and $\boldsymbol{\Phi}(\tau_f,\tau_0)$ is the state transition matrix from time τ_0 to τ_f. The MMD policy is the guidance policy that is utilized for information gathering purposes.

4. INFORMED STATION KEEPING

The objective of station keeping is to return the agent spacecraft to a desired point. The objective of information gathering for optics is to minimize range uncertainty. To combine the objectives, we seek the station keeping maneuver which minimizes range uncertainty. Thus, there must be a set of acceptable the station keeping maneuvers such that a minima can exist. If there is only a single station keeping maneuver, then the optimal solution is simply the single point. If a set of acceptable maneuvers does exist, then the objective of informed station keeping is to find the maneuver in the station keeping set which minimizes the cost function. For the purposes of this paper, which considers optical-only measurements, the cost function to minimize is range variance projection of the state estimate given by J_ρ.

The developed guidance strategy is tested in a scenario to mimic proximity operations about the Lunar Gateway. To approximate cislunar dynamics we use the CR3BP, with the equations of motion given in Section 3.2. In the CR3BP model, the target spacecraft is placed on a near rectilinear halo orbit (NRHO) with a 9:2 resonance with the lunar synodic cycle, which is currently the selected orbit for NASA's Lunar Gateway. The agent spacecraft is located on a QPO about the 9:2 NRHO with the same base frequency. Giving the agent and target the same base frequency ensure naturally bounded relative motion, which is ideal for observation and staging before further action. The average range between the natural trajectories of two spacecraft for the outlined mission is 215 km.

4.1 Combined Information Gathering and Station Keeping

Conceptually, combining station keeping and information gathering is achieved by projecting the guidance policy $\pm\boldsymbol{u}_y$ onto a surface of candidate station keeping maneuvers $\boldsymbol{u}_{sk}$. Then, the station keeping maneuver which is most aligned with the guidance policy is selected as the informed station keeping maneuver which is denoted $\boldsymbol{u}*$. To check alignment, we calculate the angle between the station keeping maneuvers and guidance policy by:

$$\theta_u = \cos^{-1}\left(\frac{\boldsymbol{u}_y^T \boldsymbol{u}_{sk}}{||\boldsymbol{u}_y^T \boldsymbol{u}_{sk}||}\right) \tag{25}$$

Because the guidance policy $\pm\boldsymbol{u}_y$ has a $\pm$, the angles $\theta_u = 0$ and $\theta_u = \pi$ must both be considered as desired solutions. To differentiate, we run a quick covariance analysis to select the better policy. The selected maneuver is then used as the informed station keeping maneuver $\boldsymbol{u}*$ which should approximately minimize range uncertainty while simaltaneously returning the agent to its desired location.

It is critical to note that guidance policy $\pm\boldsymbol{u}_y$ which is used here, is a solution to a surrogate cost function. Because it is a surrogate function the final uncertainty will only approximates the optimal solution. The loss of optimality comes with exponentially faster computation time, because the surrogate function results in an analytic linear problem, making it suitable for online computation.

4.2 Surface Station Keeping

As mentioned, the station keeping policy must contain a set of maneuvers. Fortunately, cislunar space contains quasi-periodic orbits (QPOs) which can provide a surface of targets instead of a single point. Thus, for the purposes of this paper, the objective of the station keeping policy is to phase the agent along the surface of a QPO. In order to arrive at a location on the QPO surface, two burns must be executed. The initial burn aims to match the position of the agent with a point on the QPO surface in the desired time. The second burn is to meet velocity matching requirements once the position has been achieved.

A QPO is topologically equivalent to a torus which, for the two dimensional case, has two parameterizing angles. Therefore, the implemented station keeping policy has two parameters to vary. For this work the QPO is parameterized with an invariant ring, which traces out a surface over time. The first parameter of the QPO surface is the initial ring angle, which is akin to a wrapping angle on a circle. The second parameter is time from apoapsis, because the initial ring is located at the equivalent of lunar apoapsis. This QPO surface composes the acceptable locations that the station keeping maneuver can return the agent to. For the given scenario described at the start of this section, the agent QPO and target NRHO are plotted about apoapsis in Figure 4.2.

By adjusting a phase of the QPO we are taking advantage of the fact that a QPO has a surface states which leads to a surface of potential maneuvers. This station keeping policy is not intended to be an ideal station keeping policy, it is simply a potential policy which produces a variety of maneuvers which can be searched over to identify information characteristics. The surface of potential maneuvers, and the informed station keeping maneuver $\boldsymbol{u}*$, for the scenario

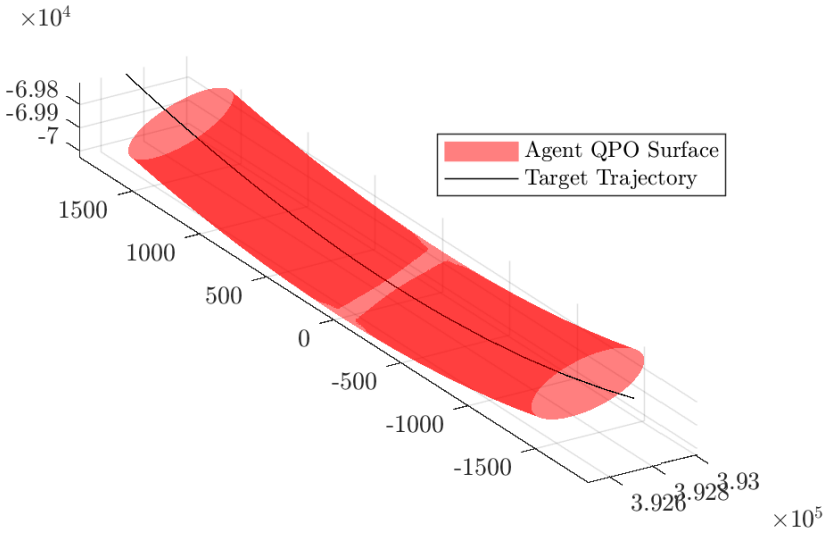

Fig. 2: Example of QPO surface which composes acceptable station keeping positions for the agent in red. This QPO is constructed about a southern L2 near rectilinear halo orbit, which represents the target trajectory in black, ensuring a closed viewing geometry.

described in the opening of this section are given in Figure 3. The left hand surface are the initial maneuvers, and the right hand plot are the secondary maneuvers. The magenta line are the informed station keeping maneuvers varied over time of arrival about apoapsis.

5. SIMULATION AND RESULTS

As described in the previous section, we seek to simulate proximity operations about the Lunar Gateway. The agent is placed on a QPO about a target on the 9:2 synodic NRHO which is the targets orbit. Both the agent and target spacecraft are estimated in a SSAT state space model and given an initial 3-σ uncertainty of 60 km and 60 cm/s per axis. The uncertainty is propagated and updated via a linear covariance analysis where the nominal trajectory is the true trajectory. The covariance analysis produces an upper bound on filter performance given that the implemented filter does not diverge from the true trajectory. The covariance analysis is deterministic and repeatable, which allows us to quickly and directly compare filter performance for each policy.

In all simulations the agent has access to optical measurements in the form of a right ascension and declination, with a root-mean-square uncertainty model as described by the measurement modeling in Section 3.3. Because we only consider optical measurements, the objective is to improve the relative range estimate as quantified by the cost J_ρ from Eq. 21. Note that the square root of the cost function $\sqrt{J_\rho}$ is the 1-σ relative range uncertainty in this case.

We simulate all of station keeping burns to construct the full solution space. The resulting final range uncertainties from the surface of maneuvers and the associated informed guidance maneuvers are all plotted in Figure 4. The surface represents the final range uncertainty $\sqrt{J_\rho}$, and the the magenta line is the informed station keeping maneuver $\boldsymbol{u}*$. The normalized phase axis is the agents secondary torus angle divided by 2π, such that 1 would be a full rotation on the torus angle. The time from apoapsis is the time the station keeping maneuver is returning the agent to the nominal QPO.

The figure depicts that the informed station keeping maneuvers do in fact fall in the valley of range uncertainty as desired, with a single point being raised by a small local peak. The small local peak near the center of the valley is induced by the secondary maneuver which is not accounted for in our prediction, but it only marginally impacts this single point. Therefore, of the full surface of potential station keeping maneuvers that are available, then the projection of the information gathering guidance policy $\boldsymbol{u}_y$ can be used to quickly select a maneuver that significantly improves state estimation as well.

Fig. 3: Surface of station keeping maneuvers, $\boldsymbol{u}_{sk}$, to phase along an agent along a QPO. The first burn is in the left plot and second burn is in the right plot. The guidance maneuver from the information gathering policy is the magenta line on the first burn.

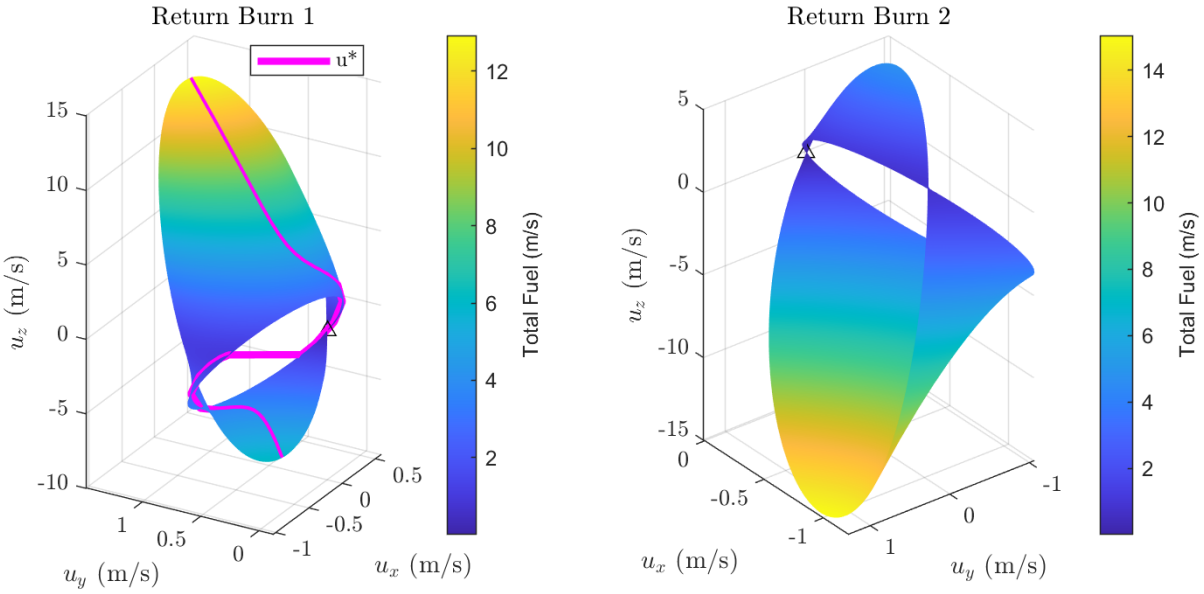

Fig. 4: Surface of all possible range uncertainties produced by station keeping maneuvers in Figure 3. The normalized phase is the second torus angle, and time from apsis is time the agent returns to the QPO surface. The informed guidance maneuvers $\boldsymbol{u}*$ are on the magenta line.

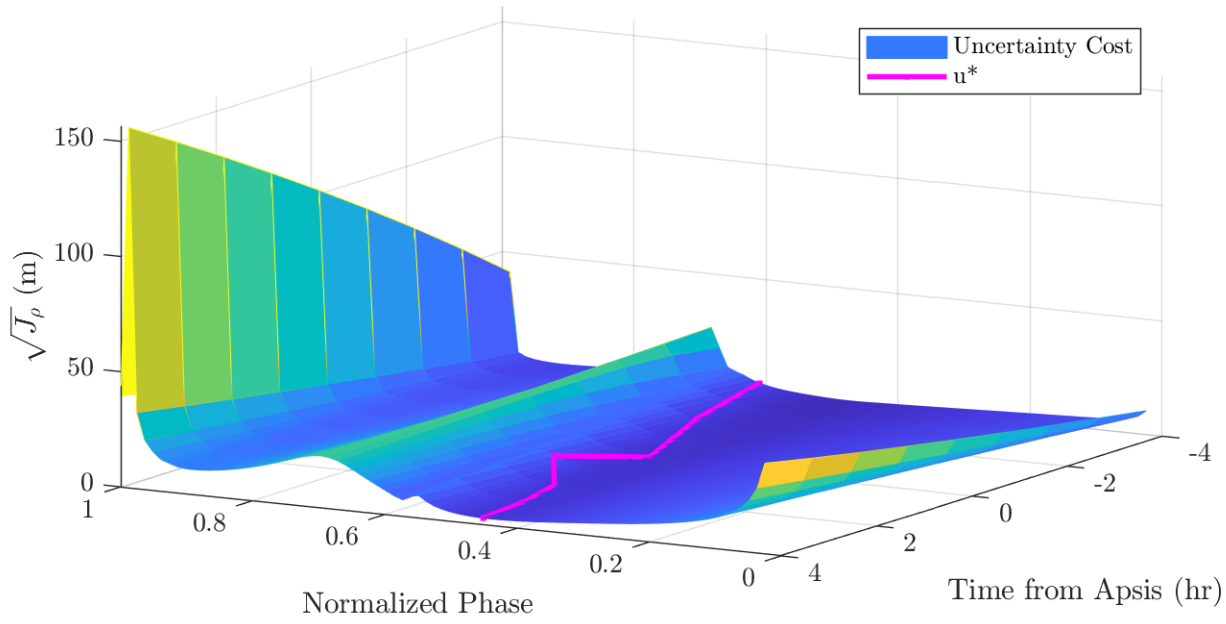

As a final analysis it is worth examining the fuel cost for these maneuvers to determine if the guidance policy selects the largest maneuvers. The total fuel costs and informed station keeping maneuvers are displayed in Figure 5. Note the time from apoapsis axis has been flipped to get a better view of the informed maneuvers. As we can see the guidance policy avoids the peak fuel cost in favor of alignment with the policy $\boldsymbol{u}_y$. Thus, it is clear this method does not simply select large maneuvers to create deviations, it looks for maneuver alignment.

Fig. 5: Surface of all possible fuel costs produced by station keeping maneuvers in Figure 3. The normalized phase is the selected torus angle, and time from apsis is the selected targeting time for the station keeping maneuvers. The predicted results from the guidance policy is the magenta line.

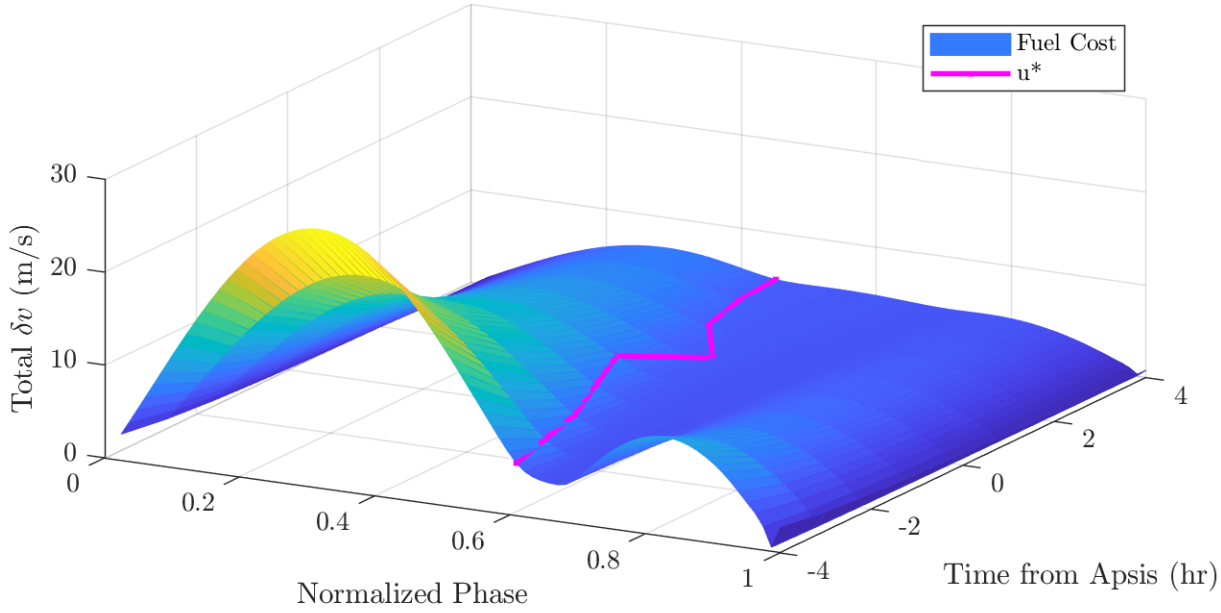

6. CONCLUSIONS

Autonomous spacecraft to spacecraft tracking using optical sensors is an exciting area of research with the potential to enable new and more robust missions. While optical sensors are a light-weight, low-power, and effective measurement source, they inherently lack range information which may take substantial time to obtain because it is only locally observable for space systems. Instead of waiting for the natural dynamics to create substantially observational changes necessary for range information to be estimated, which may take on the time scale of orbit periods, one satellite may preform a maneuver to change the relative geometry to obtain new state information. Gathering information to reduce uncertainty is critical to systems which desire to perform autonomous operations. By extension the developed guidance methods should be low-computation cost to fit within the autonomous framework.

We have combined information gathering with station keeping by projecting an autonomous guidance policy onto a station keeping set. The station keeping maneuver which most aligns with the guidance maneuver is selected as the informed station keeping maneuver. This informed maneuver is able to return the agent spacecraft to a desired location while significantly improve range information. It must be noted that while the station keeping maneuvers themselves are not fuel optimal, they can be replaced with a more complex and lower cost set if found.

There are several avenues for future work. First, maneuver execution errors should be included and measured with accelerometers to determine the level of accuracy necessary for the maneuver/sensor to ensure noisy does not overtake the information gain. Second, alternative station keeping policies that produce lower fuel costs should be examined.

Finally, these guidance maneuvers should be simulated in a full filter simulation to determine filter consistency.

[1] Nicholas Bradley, Zubin Olikara, Shyam Bhaskaran, and Brian Young. Cislunar navigation accuracy using optical observations of natural and artificial targets. *Journal of Spacecraft and Rockets*, 57(4):777–792, 2020.

[2] Pedro Rocha Cachim, João Gomes, and Rodrigo Ventura. Autonomous orbit determination for satellite formations using relative sensing: Observability analysis and optimization. *Acta Astronautica*, 200:301–315, 2022.

[3] Michele Ceresoli, Giovanni Zanotti, and Michèle Lavagna. Bearing-only navigation for proximity operations on cis-lunar non-keplerian orbits. In *72nd International Astronautical Congress (IAC 2021)*, pages 1–10, 2021.

[4] Raja Jon Vurputoor Chari. *Autonomous orbital rendezvous using angles-only navigation*. PhD thesis, Massachusetts Institute of Technology, 2001.

[5] Fabio D'Onofrio, Giordana Bucchioni, and Mario Innocenti. Bearings-only guidance in cis-lunar rendezvous. *Journal of Guidance, Control, and Dynamics*, 44(10):1862–1874, 2021.

[6] Jesse A Greaves and Daniel J Scheeres. Observation and maneuver detection for cislunar vehicles: Using optical measurements and the optimal control based estimator. *The Journal of the Astronautical Sciences*, 68(4):826–854, 2021.

[7] Jesse A Greaves and Daniel J Scheeres. Absolute and autonomous navigation for distributed space systems from relative measurements. In *33rd AAS/AIAA Space Flight Mechanics Meeting*, 2023.

[8] Jesse A Greaves and Daniel J Scheeres. Autonomous information gathering guidance for distributed space systems with optical sensors. In *2023 American Controls Conference*, 2023.

[9] Jonathan Grzymisch and Walter Fichter. Analytic optimal observability maneuvers for in-orbit bearings-only rendezvous. *Journal of Guidance, Control, and Dynamics*, 37(5):1658–1664, 2014.

[10] Sherry Elizabeth Hammel. *Optimal observer motion for bearings-only localization and tracking*. University of Rhode Island, 1988.

[11] James P Helferty and David R Mudgett. Optimal observer trajectories for bearings only tracking by minimizing the trace of the cramer-rao lower bound. In *Proceedings of 32nd IEEE Conference on Decision and Control*, pages 936–939. IEEE, 1993.

[12] Keric A Hill. *Autonomous navigation in libration point orbits*. PhD thesis, University of Colorado at Boulder, 2007.

[13] Evan Kaufman, T Alan Lovell, and Taeyoung Lee. Nonlinear observability for relative orbit determination with angles-only measurements. *The Journal of the Astronautical Sciences*, 63:60–80, 2016.

[14] Jun'ichiro Kawaguchi, Tatsuaki Hashimoto, Takashi Kubota, Shujiro Sawai, and Gene Fujii. Autonomous optical guidance and navigation strategy around a small body. *Journal of guidance, control, and dynamics*, 20(5):1010–1017, 1997.

[15] Jackson Kulik and Dmitry Savransky. State transition tensors for passive angles-only relative orbit determination. In *33rd AAS/AIAA Space Flight Mechanics Meeting*, 2023.

[16] Yong Li and Ai Zhang. Observability analysis and autonomous navigation for two satellites with relative position measurements. *Acta Astronautica*, 163:77–86, 2019.

[17] F Markley. Autonomous navigation using landmark and intersatellite data. In *Astrodynamics conference*, page 1987, 1984.

[18] Sung-Hoon Mok, Jaehwan Pi, and Hyochoong Bang. One-step rendezvous guidance for improving observability in bearings-only navigation. *Advances in Space Research*, 66(11):2689–2702, 2020.

[19] Steven C Nardone and Vincent J Aidala. Observability criteria for bearings-only target motion analysis. *IEEE Transactions on Aerospace and Electronic systems*, (2):162–166, 1981.

[20] Yangwei Ou, Hongbo Zhang, and Bin Li. Absolute orbit determination using line-of-sight vector measurements between formation flying spacecraft. *Astrophysics and Space Science*, 363(4):1–13, 2018.

[21] Jean-Michel Passerieux and Dominique Van Cappel. Optimal observer maneuver for bearings-only tracking. *IEEE Transactions on Aerospace and Electronic Systems*, 34(3):777–788, 1998.

[22] Mark L Psiaki. Autonomous orbit determination for two spacecraft from relative position measurements. *Journal of Guidance, Control, and Dynamics*, 22(2):305–312, 1999.

[23] Fabrizio Schiano and Roberto Tron. The dynamic bearing observability matrix nonlinear observability and estimation for multi-agent systems. In *2018 IEEE International Conference on Robotics and Automation (ICRA)*, pages 3669–3676. IEEE, 2018.

[24] David Smitherman and Andrew Schnell. Gateway lunar habitat modules as the basis for a modular mars transit habitat. In *2020 IEEE Aerospace Conference*, pages 1–12. IEEE, 2020.

[25] Joshua Sullivan, Adam W Koenig, Justin Kruger, and Simone D'Amico. Generalized angles-only navigation architecture for autonomous distributed space systems. *Journal of Guidance, Control, and Dynamics*, 44(6):1087–1105, 2021.

[26] Shota Takahashi and Daniel J Scheeres. Autonomous exploration of a small near-earth asteroid. *Journal of Guidance, Control, and Dynamics*, 44(4):701–718, 2021.

[27] Evan M Ward and Roshni J Patel. On the observability of spacecraft navigation using landmarks. In *2022 IEEE Aerospace Conference (AERO)*, pages 1–14. IEEE, 2022.

[28] David C Woffinden and David K Geller. Observability criteria for angles-only navigation. *IEEE Transactions on Aerospace and Electronic Systems*, 45(3):1194–1208, 2009.

[29] David C Woffinden and David K Geller. Optimal orbital rendezvous maneuvering for angles-only navigation. *Journal of guidance, control, and dynamics*, 32(4):1382–1387, 2009.